Photoelectrochemical Investigations on Naphthalocyanine Derivatives in Thin Films

Hisao Yanagi,* Yoshihiro Kanbayashi, Derck Schlettwein,†,‡ Dieter Wöhrle,† and Neal R. Armstrong‡

Faculty of Engineering, Kobe University, Rokkodai, Nada, Kobe 657, Japan, Organische und Makromolekulare Chemie, Universität Bremen, Postfach 330440, D-28334 Bremen, Germany, and Department of Chemistry, The University of Arizona, Tucson, Arizona 85721

Received: November 17, 1993; In Final Form: February 22, 1994®

Photoelectrochemical properties of Zn–naphthalocyanine (ZnNc) and its modified compound, Zn–2,3-tetraquinoxalinotetraazaporphyrin (ZnTQP) were investigated in thin films. The ZnNc electrode vacuum-deposited on an indium tin oxide (ITO) substrate exhibited almost an ohmic I–V curve in the dark and small cathodic photocurrents under illumination, which was typical for the p-type semiconduction of the ZnNc layer, in a photoelectrochemical cell. The drop-casted film electrode of ZnTQP, on the other hand, showed rectified I–V characteristics in the dark and high anodic photocurrents under illumination, which was attributed to the n-type semiconducting character of the ZnTQP layer. These different photoelectrochemical behaviors were characterized by photocurrent action spectra and ultraviolet photoelectron spectroscopy. The substitution with quinoxalino groups into the Nc macrocyclic system gave rise to lowering of the HOMO energy level for the TQP molecule. This electronic energy shift generated donor electron states in the band gap after contact with the substrate or electrolyte and enabled the photooxidation at the valence band edges corresponding to the Soret- and Q-band excitations. The pH dependence of the anodic photocurrents for the ZnTQP electrode indicated that the photooxidation occurred through a hole injection from the HOMO and underlying sub-HOMO states, separately, for the Soret- and Q-band excitations. For the ZnNc electrode, the Q-band illumination produced cathodic photocurrents, whereas the Soret band produced anodic photocurrents. It suggested that under the Soret-band excitation holes generated in the sub-HOMO state directly contributed to the photooxidation.

Introduction

Solar light conversion is one of the most pressing needs for a future energy technology. Intensive works have attained highly efficient solar cells using inorganic silicon semiconductors with a narrow band gap.[1] Another approach to solar energy conversion has been attempted to develop a photosynthetic model.[2] Some organic molecular dyes such as porphyrins and phthalocyanines (Pcs)[3-5] are anticipated to realize it because of their molecular characteristics analogous to chlorophyll in the photosynthetic system. Molecular semiconducting properties of those molecules sensitive to solar irradiation have been utilized for sensitization of wide band-gap semiconductors,[6,7] organic photovoltaic cells,[8-11] and photoelectrochemical systems with dye-modified electrodes.[11-15] Most of porphyrins and Pcs have been characterized as p-type molecular semiconductors[16,17] from the rectifying behavior in the Schottky-type contact with metals and the photocathodic reaction at an interface with electrolytes.[11-17] Their p-type semiconduction is attributed to a spontaneous doping of ambient oxygen into the dye layers.[15,16,18-20] Charge transfer from dye molecules to oxygen gives rise to acceptor states within the band gap. Conductivity and photoconductivity of molecular semiconductors consequently are discussed as extrinsic properties.[21] Thin films of ZnPc or ZnNc as prepared under ultrahigh vacuum (UHV) conditions behave as insulators. The electrical conductivity in the dark and also the photoconductivity increase during exposure to oxygen. The opposite is found for films of n-type materials like perylene[9] pigments or Zn–tetrapyridotetraazaporphyrin,[17] an aza analogue of ZnPc. Their relatively high initial conductivity also is discussed in terms of impurities and imperfections introduced during the film preparation. Intrinsic values of the conductivity are expected to be extremely low in view of the small bandwidth[22] of molecular semiconductors. The formation of charge-transfer complexes with donors or acceptors is dominated by the electronic energy potential of dye molecules. A modification of the molecular structure enables the energy level of molecular orbitals to change,[17,23,24] which consequently implies a possibility to control the conduction type of molecular semiconductors.

The previous work of chemically modified Pcs[17,25] has demonstrated that the electrodes of tetrapyrido- and tetrapyrazinotetraazaporphyrins exhibit photooxidation of a suitable donor under illumination with visible light, contrary to the typical photoreduction of a suitable acceptor at the electrode of unsubstituted Pc, in a photoelectrochemical cell. This opposite photoelectrochemical behavior was interpreted in terms of a band energy shift to lower potentials for the tetraazaporphyrin macrocycles, which was caused by substitution with electron-withdrawing pyrido and pyrazino groups. A similar change of molecular semiconducting properties has been reported about substitution with pyridyl groups into tetraphenylporphyrin in a photovoltaic cell.[26] These semiconducting behaviors of substituted porphyrins noteworthily suggest the possibility of organic materials for heterojunctions photovoltaic cells and photoelectrochemical cells sensitive to solar light.

As well as introduction of substituted groups, the molecular framework of macrocycles influences their semiconducting characteristics.[8,10] For efficient conversion of solar energy, the dye molecules are preferred to have a wide absorption in the visible light range. In general, a more extended π-electron conjugated system groing from porphyrin to Pc macrocycles brings about a shift of absorption maxima to the longer wavelengths,[3-5] which results in a light harvest better matched with the solar spectrum. To sensitize in the near infrared region (700–900 nm), a further benzoannelation is introduced into Pc rings, which results in naphthalocyanine (Nc) derivatives.[5,27-30] Metal Ncs (MNcs, Figure 1a), therefore with narrower band gaps than Pcs, have attracted much interest in their applications to optical data recording and electrophotography sensitive to semiconductor lasers,[31,32] as well as solar energy conversion.[10] Besides a utilization of the longer-wavelength region in solar light, the modified structure with the large macrocyclic system of MNc

† Universität Bremen.
‡ The University of Arizona.
® Abstract published in *Advance ACS Abstracts*, April 1, 1994.

0022-3654/94/2098-4760$04.50/0

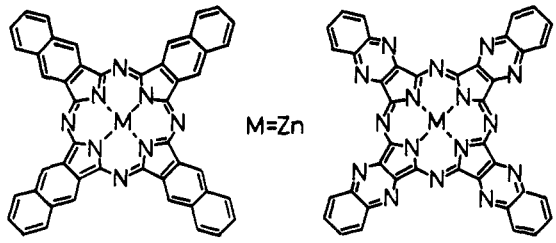

Figure 1. Molecular structures of zinc complexes of naphthalocyanine (a, ZnNc) and 2,3-tetraquinoxalinotetraazaporphyrin (b, ZnTQP).

probably provides an absolute electronic energy shift of both occupied and unoccupied states. Such a band energy shift may again involve a variety of preferable contacts between these dye molecules and metals or electrolytes in a photocell. However, only few investigations have so far been made on photovoltaic and photoelectrochemical behaviors of MNcs.

This work was performed to clarify the molecular semiconducting nature of MNcs and their derivatives by means of photoelectrochemical measurements in comparison to metal Pc (MPc) analogues. Substitution with quinoxalino groups into the Nc ligand provided 2,3-tetraquinoxalinotetraazaporphyrin (TQP, Figure 1b) as a modified Nc to study the effect of electron-withdrawing substituents in Nc as compared to the situation in Pc.[17] Zinc complexes of Nc and TQP were chosen to prepare dye-coated electrodes for photoelectrochemical investigations. Current–voltage characteristics and photocurrent action spectra of the thin film electrodes were examined in a photoelectrochemical cell. Opposite responses, cathodic photocurrents at the ZnNc electrode and anodic photocurrents at the ZnTQP electrode under visible light illumination are discussed in terms of different configurations of their band energies. The change in the electronic energy states of the molecules caused by substitution with quinoxalino groups into the Nc-ligand was demonstrated by means of visible (VIS) spectroscopy and ultraviolet photoelectron spectroscopy (UPS).

Experimental Section

ZnNc was prepared by slight modification of a described procedure.[30,33] 2,3-Dicyanonaphthalene (0.5 g, 2.8 mmol) and zinc acetate (0.13 g, 0.7 mmol) were mixed and sealed in an evacuated glass tube after being flushed with nitrogen gas. After the tube was heated at 250 °C for 4 h, the crude powder was stirred in 0.01 M HCl in order to dissolve unreacted zinc acetate. The product was filtered, washed with water, followed by an exhaustive Soxhlet extraction with acetone, and dried at 100 °C in vacuo. For synthesis of ZnTQP, 2,3-dicyanoquinoxaline was synthesized by slight modification of a known method.[34] A mixture of *o*-phenylenediamine (0.1 g, 9.5 mmol) and diiminosuccinonitrile (1.0 g, 9.5 mmol) was gradually added into 50 mL of trifluoroacetic acid and heated at 45 °C for 2 h under nitrogen. After the solvent was evaporated, the product was neutralized with dilute HNO_3, washed with water, and dried at 100 °C in vacuo. ZnTQP was synthesized from prepared 2,3-dicyanoquinoxaline and zinc acetate in accordance with the procedure for ZnNc.

Thin film electrodes of ZnNc and ZnTQP were prepared by deposition onto indium tin oxide (ITO) conductive glass substrates (10 × 12 mm, Central Glass Co. Ltd.). ZnNc was vacuum-deposited on ITO kept at room temperature from a quartz crucible heated with a tungsten coil in a vacuum of 5×10^{-4} Pa using a JEOL JEE-4X vacuum-evaporator, according to the previous procedure.[33] The deposition rate and film thickness were regulated at 5 nm min^{-1} and 100 nm, respectively, using a quartz crystal microbalance. ZnTQP, which could not be sublimed in a vacuum, was processed into thin films by a drop-casting technique.[19,25] A solution of 3.6 g L^{-1} ZnTQP in *N*,*N*-dimethylacetamide (DMA) was dropped onto ITO and dried at 60 °C in vacuo. The film thickness of ZnTQP was controlled to be ca. 100 nm by estimating from the extinctions at the absorption maxima.

Photoelectrochemical measurements were performed in a gas-tight 20-mL cell using a conventional three-electrode system with a coiled platinum wire as a counter and an Ag/AgCl (saturated KCl) reference electrode.[17,25] An electrical contact to the working electrodes of ZnNc and ZnTQP was made to the ITO substrate with a glass-covered copper wire and a silver conducting paste and sealed with an epoxy resin to maintain an electroactive area of 1 cm^2. The electrolyte used was 0.5 M KNO_3 including a redox couple of 1 mM *p*-hydroquinone(HQ)/*p*-benzoquinone(BQ). By addition of HNO_3 or KOH, the pH values of electrolyte solutions were changed in a range from 2.2 to 11.0. The electrolyte solution was deoxygenated by purging with argon gas before measurements. Current–voltage (I-V) characteristics in the dark and under illumination were measured using a Hokuto Denko HA-301 potentiostat and a HB-104 function generator at a constant scan rate of 5 mV s^{-1}. White light of 100 mW cm^{-2} was illuminated through a 5-cm water filter with a Shimadzu AT-100HG halogen lamp. The illumination was performed from both the organic layer (front side) and the ITO substrate (back side) through quartz windows of the cell. Dependence of photocurrents on the wavelength was measured using interference filters with a Toshiba XS-500 xenon lamp light source. Photocurrent action spectra were obtained by normalizing the monochromatic light incidence at 1 mW cm^{-2}. The incident light intensity was controlled using an Advantest TQ8215 optical power multimeter.

UPS experiments were performed using a Vacuum Generators Escalab MkII spectrometer. Spectra were collected using He I radiation (21.2 eV) from a capillary discharge lamp. The retarding grid of the hemispherical analyzer was kept at voltages corresponding to a constant retard ratio of 4 to increase sensitivity in the region of lowest binding energies. Before a spectrum was taken, a polycrystalline gold (99.99%, Aldrich) surface was rinsed in methanol and water before treatment with an argon ion beam until it was atomically clean as controlled by X-ray photoelectron spectroscopy (XPS) and UPS spectra. The samples were prepared by a vacuum deposition for ZnNc and a mechanical press of powder for ZnTQP on the gold surface in a way that the gold spectrum was still visible to have a calibration for the sample spectrum.[21]

Visible (VIS) absorption spectra of ZnNc and ZnTQP were recorded in DMA solutions and in thin films deposited on ITO using a Shimadzu UV-2200 spectrometer. The morphology of the prepared electrodes was examined by scanning electron microscopy (SEM). The thin films deposited on ITO substrates were coated with a vacuum-evaporated gold film. The observation was carried out at 20-kV acceleration using a Hitachi S-2500 scanning electron microscope.

Results

Characterization of Electrode Materials. ZnNc was easily processed in thin films by vacuum deposition, whereas ZnTQP could not be vacuum-evaporated under the employed condition. ZnTQP was also less soluble in most organic solvents than ZnNc. Such different characteristics can be attributed to a change in their molecular interaction caused by substitution with quinoxalino groups into the Nc ligand. In the TQP macrocyclic ligands a delocalization of π-electrons in the conjugated Nc-ring system is partly distorted at the introduced nitrogen atoms. This partial localization of π-electrons might increase an electrostatic interaction between adjacent TQP molecules, which would result in the impracticable vacuum evaporation and less solubility. Therefore, ZnTQP could be dissolved only in a polar solvent; thus a drop-casted film of ZnTQP was prepared from a DMA solution. Figure

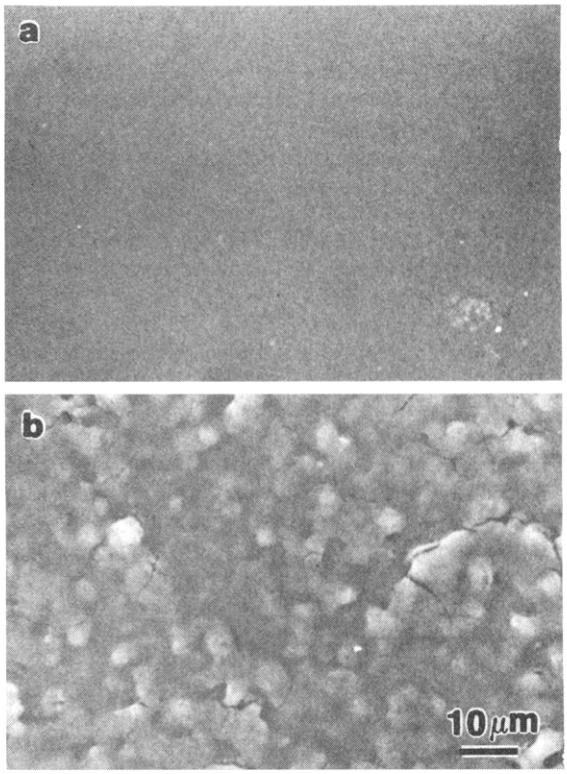

Figure 2. Scanning electron micrographs of vacuum-deposited ZnNc film (a) and drop-casted ZnTQP film (b).

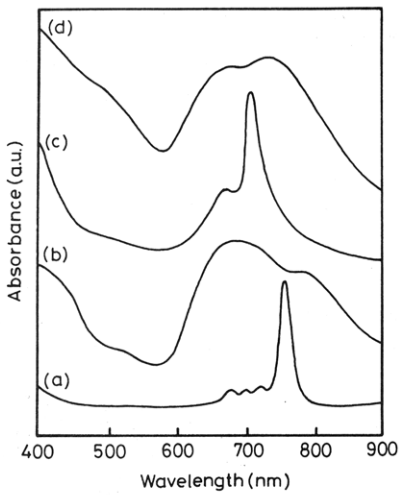

Figure 3. Visible absorption spectra of ZnNc (a,b) and ZnTQP (c,d): (a,c) in DMA solution, (b) vacuum-deposited film, and (d) drop-casted film.

2 shows SEM photographs of the electrodes of vacuum-deposited ZnNc and drop-casted ZnTQP films. The morphology of the ZnNc film was very smooth (Figure 2a), while ZnTQP precipitated in a rugged film composed of particles of 5–10 mm in size (Figure 2b). The low solubility of ZnTQP causes a fast aggregation of molecules into such inhomogeneous grains. From the different morphology of the films it becomes clear that no quantitative comparison between the ZnNc and ZnTQP electrodes can be drawn from the absolute height of the observed photocurrents mentioned in the following section. However, information about electrical properties of the electrode materials can be obtained, mainly from the direction of the photocurrent, also under different illumination conditions.

Figure 3 shows VIS spectra of the vacuum-deposited ZnNc and drop-casted ZnTQP films, together with their solution spectra in DMA. ZnNc exhibits a sharp absorption maximum (λ_{max}) at 758 nm in solution (Figure 3a) which is assigned to the Q-band, a π–π^* transition of the macocyclic Nc ligand.[5,35] The λ_{max} of ZnNc is considerably higher than that obtained for ZnPc, 668 nm.[25] The extension of the π-electron conjugating ligand system from Pc to Nc causes lowering of a transition energy between the HOMO and LUMO levels of the molecule. The vacuum-deposited film of ZnNc indicates broad absorption bands around 690 and 790 nm, in which the absorbance of the former band is higher than that of the latter (Figure 3b). Similar spectral features have been studied for vacuum-deposited films of MPcs, and the spectra with such relative absorbances are assigned to the metastable α-polymorphic form of MPc crystals.[15,36,37] The structural observations of the ZnNc film by high-resolution electron microscopy and scanning tunneling microscopy[33,38,39] have demonstrated that the ZnNc molecules are piled up in a columnar packing that is similar to those well-known for MPc crystals. From this analogy to MPc, the vacuum-deposited ZnNc likely crystallizes in the same metastable form as in the α-MPc film.

The solution spectrum of ZnTQP exhibits λ_{max} at 708 nm (Figure 3c), which is significantly lower than that, 758 nm, of ZnNc. The π–π^* transition of the Q-band specifically involves charge transfer from the outer annelated aromatic rings to the inner macrocyclic ring.[40] Therefore, some localization of conjugating π-electrons at the electronegative N-atoms in the TQP ligand caused by substitution with quinoxalino groups widens the HOMO–LUMO energy gap. Such a tendency has been demonstrated also for substituted Pc derivatives.[25] An introduction of nitrogen atoms into the Pc ligand, i.e. substitution with pyrido and further pyrazino groups, resulted in a blue shift of λ_{max} in their solution VIS spectra. The width of the absorption region of the Q-band spectrum in ZnTQP solution is rather broad as compared to that of ZnNc. This can be attributed to some molecular aggregation in solution wihch results from the increased intermolecular interaction due to the substitution with quinoxalino groups. The VIS spectrum of the drop-casted ZnTQP film exhibits a broad Q-band absorption with two maxima around 670 and 745 nm (Figure 3d). Such split absorption bands suggest a columnar stacking structure similar to the ZnNc film; however, the relative intensity of the two bands is inversed as compared to ZnNc (Figure 3b). This spectrum of the ZnTQP film indicates that ZnTQP molecules crystallize in a stable polymorphic form which is known for β-form MPc crystals grown from a solution.[15,36,37] A similar feature of absorption spectra of thin films obtained by vapor deposition or coating has been described for phthalocyanine and tetraazaporphyrin derivatives.[15,25,34]

In order to discuss the different photoelectrochemical behavior of the dye-coated electrodes, as presented below, a knowledge of the position of energy levels in the solid state is crucial. This is necessary not only to understand processes at each electrode surface in contact with the electrolyte but also to describe the nature of the back-contact toward the ITO electrode. Therefore UPS has been performed at thin films of the samples on atomically clean gold whose Fermi edge was used as an internal calibration of the spectra. In Figure 4 the spectra of ZnNc and ZnTQP are presented as referred to the gold Fermi edge. The gold work function had been determined independently to be 5.02 eV.[21] It is seen that the molecular modification from ZnNc to ZnTQP brings about a change not only in the frontier orbital gap as described above (Figure 3) but also in the absolute position of the HOMO. In analogy to UPS and XPS measurements for MPcs,[14,41–44] the first ionization is considered to correspond to an electron removal from the HOMO π-level of the Nc and TQP macrocyclic ligand. The HOMO level of ZnTQP is found to be located about 0.9 eV below that of ZnNc. Energy calculations for modified Pc and tetraazaporphyrin macrocycles have demonstrated that the substitution with electron-withdrawing groups and nitrogen-containing heterocyclic rings gives rise to lowering of electronic energies in both the HOMO and LUMO levels.[23,24] In electrochemical experiments this trend could be confirmed by

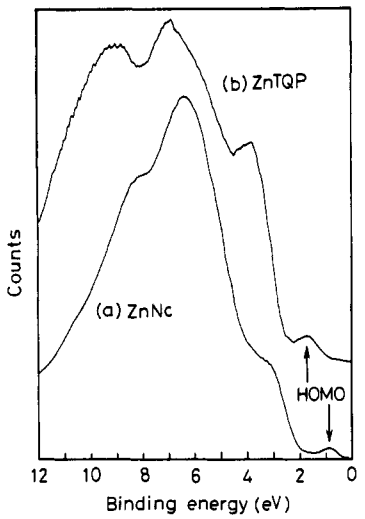

Figure 4. Ultraviolet photoelectron spectra (He(I)) of ZnNc (a) and ZnTQP (b) as compared to the Fermi edge of the gold substrate.

a more positive potential of reduction of those complexes containing electron-withdrawing ligands and substituents.[45] The valence electrons of the Nc ligand are delocalized in the π-conjugating macrocylic ring, as suggested by the sharp Q-band VIS spectrum of ZnNc (Figure 3a). The substitution with quinoxalino groups causes some electron stabilization at the introduced nitrogen atoms in the TQP molecule, which shifts analogously the HOMO electron level to lower energy. Such an energy shift in the electronic states significantly influences also their molecular semiconducting properties, which dominate the photoelectrochemical behaviors of the dye-coated electrodes, as discussed in the subsequent section. The ionizations with higher binding energies in Figure 4 are explained by orbitals composed of both carbon and nitrogen atoms in the macrocyclic ligand and the central Zn metal. The valence electron spectra in this binding energy region of MPcs in XPS[46] have been assigned to the orbitals formed by a coordination of the metal d-electrons with the four central nitrogens of the Pc ligand. The spectra of ZnNc and ZnTQP show very similar patterns. In general the bands of ZnNc are shifted to higher electron energies (lower binding energies) as compared to ZnTQP (Figure 4). Such valence spectral features can be attributed to the different coordination natures between the Nc and TQP macrocyclic ligands with the central Zn metal.

Photoelectrochemical Behaviors. The prepared electrodes of the vacuum-deposited ZnNc and drop-casted ZnTQP films on ITO substrates were examined in a photoelectrochemical cell with an aqueous electrolyte of 0.5 M KNO_3 including a redox couple of 1 mM HQ/BQ. The pH value of the electrolyte solution after deoxygenation by purging with argon was 4.3. It was confirmed, before the measurements, that the bare ITO substrate exhibited no prominent redox peak in the measured potential ranges.

Figure 5 shows I–V curves of the ZnNc electrode in the dark and under illumination from the front and back sides with 100 mW cm^{-2} white light. The dark currents change almost proportionally to the positive and negative voltages applied with respect to the rest potential (E_{rest} = 0.37 V vs Ag/AgCl), which is defined as an equilibrium potential in the dark. This I–V characteristic is not like the previous measurement on the vacuum-deposited ZnPc electrode which exhibited a clear rectifying curve in the same electrochemical condition.[25] Its higher dark currents rectified at the anodic potentials were interpreted by a typical blocking contact of the p-type semiconducting ZnPc layer with the electrolyte solution. Under illumination the blocking contact formed at the ZnPc surface produced cathodic photocurrents of -14 μA cm^{-2} at E_{rest}. The present ZnNc electrode also exhibits cathodic photocurrents under illumination, however, which are very small as compared to those of the ZnPc electrode. The

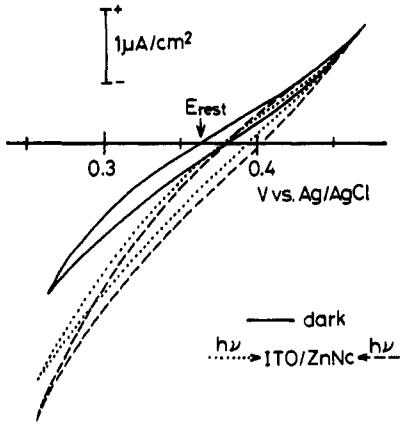

Figure 5. Current–voltage curves for ITO/ZnNc electrode in the dark (solid line) and under illumination with 100 mW cm^{-2} white light from front side (dashed line) and back side (dotted line), in 0.5 M KNO_3 and 1 mM HQ/BQ at pH 4.3.

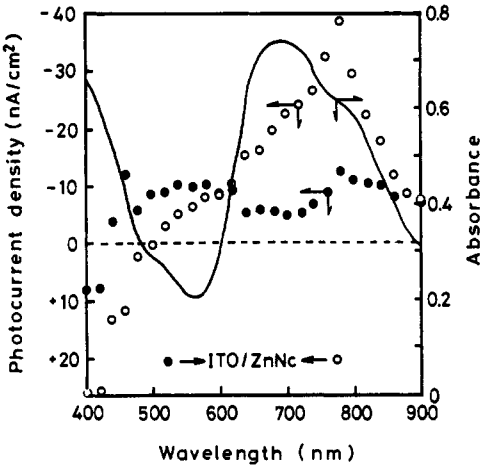

Figure 6. Photocurrent action spectra for ITO/ZnNc electrode at 0.37 V vs Ag/AgCl, pH 4.3, under illumination from front side (○) and back side (●), and its absorption spectrum (solid line). Photocurrents were normalized with monochromatic light intensity of 1 mW cm^{-2}.

photocurrents of ZnNc at the cathodic potentials are a little higher for the front-side illumination than for the back-side one.

Such a difference depending on the illuminated sides is clearly seen in their photocurrent action spectra taken at E_{rest} (0.37 v vs Ag/AgCl), as is shown in Figure 6. The cathodic photocurrents under the front-side illumination increase in the Q-band absorption region (700–800 nm). On the other hand, under the back-side illumination the photocurrents in the Q-band region decrease, whereas photocurrents at 500–600 nm, where the absorption spectrum falls, are rather higher. This dependence of photocurrents on the wavelengths under the back-side illumination suggests a filtering effect.[47,48] of the ZnNc layer. Therefore, a photoactive interface is formed at the front-side contact with the electrolyte solution, and ZnNc shows p-type semiconducting characteristics, which is likewise the case for the ZnPc electrode. However, the small photocurrents and less rectifying I–V characteristics of the ZnNc electrode suggest a modified nature of the contact with electrolytes. As pointed out in the previous section, the extension of the conjugated macrocyclic ligand from Pc to Nc results in an energy shift of electronic states of the molecules. It is generally expected that the π-electron-rich Nc ligand is in a higher electronic potential than Pc.[23] However, to form a blocking contact between the p-type organic layer and the electrolyte solution, the Fermi level of the molecular semiconductor should lie below the redox potential of the containing redox couple. Therefore, the higher energy states of ZnNc is unfavorable for the blocking contact formation, and seems to make the contact rather ohmic.

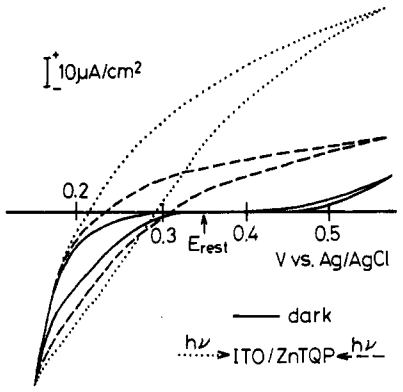

Figure 7. Current–voltage curves for ITO/ZnTQP electrode in the dark (solid line) and under illumination with 100 mW cm^{-2} with light from front side (dashed line) and back side (dotted line), in 0.5 M KNO_3 and 1 mM HQ/BQ at pH 4.3.

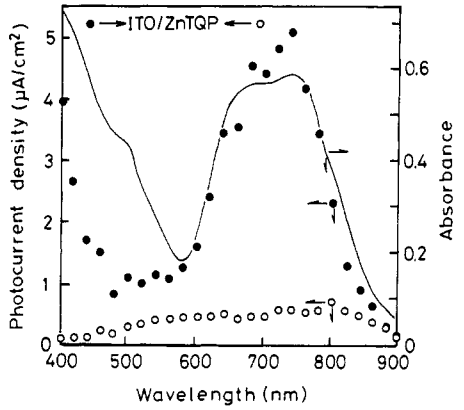

Figure 8. Photocurrent action spectra for ITO/ZnTQP electrode at 0.35 V vs Ag/AgCl, pH 4.3, under illumination from front side (○) and back side (●), and its absorption spectrum (solid line). Photocurrents were normalized with monochromatic light intensity of 1 mW cm^{-2}.

Furthermore, it should be noted about the photocurrent action spectra of ZnNc (Figure 6) that illumination produces anodic photocurrents in the short-wavelength region around 400 nm in both the front-side and back-side modes. The VIS absorption spectrum of the ZnNc electrode (Figure 6) indicates an intense absorption at this wavelength region, which is designated as the Soret band due to another π–π^* transition from an analogy to VIS spectra of MPcs, along with the Q-band absorption.[3,5] It is therefore suggested that the photoreduction and photooxidation occur through separated processes corresponding to the Q-band and Soret-band excitations, respectively. The quantum yield for photocurrents against the absorbed monochromatic light at 780 and 400 nm was calculated to be 7.95×10^{-3} and 1.03×10^{-2}%, respectively, under the front-side illumination.

Figure 7 shows I–V characteristics of the ZnTQP film electrode drop-casted on ITO. In the dark the electrode exhibits a remarkable rectifying curve, in which high dark currents appear when negative potentials are applied with respect to E_{rest} (0.35 V vs Ag/AgCl). The illumination with white light produces anodic photocurrents, contrary to the cathodic photocurrents for the ZnNc electrode. The photocurrents obtained at E_{rest} under the back-side illumination, 36 μA cm^{-2}, are significantly higher than that, 12 μA cm^{-2}, under the front-side illumination. This photoelectrochemical response of ZnTQP is quite opposite to those for p-type semiconducting MPcs blocking-contacted with electrolytes, but it is similar to photooxidation behaviors observed for substituted tetrapyrido- and tetrapyrazinotetraazaporphyrin electrodes.[17,25] In Figure 8 photocurrent action spectra of the ZnTQP electrode taken at E_{rest} (0.35 V vs Ag/AgCl) are shown for the illumination from both sides. The back-side illumination produces high anodic photocurrents corresponding well to the

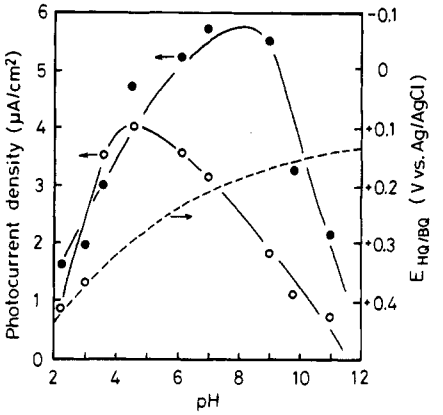

Figure 9. Dependence of photocurrents for ITO/ZnTQP electrode on pH of electrolyte under monochromatic illumination (1 mW cm^{-2}) at the Soret-band (400 nm) (○) and the Q-band (680 nm) (●) absorptions, with redox potential change of HQ/BQ electrolyte (dashed line).

Q-band and Soret-band absorption spectra, while under the front-side illumination the photocurrents are very small over the wavelength range. This result indicates, in contrast to ZnNc, that photoexcited ZnTQP molecules near the contact with the ITO substrate efficiently contribute to the photooxidation reaction. To produce the anodic photocurrents, excitons should separate into charge carriers which are transported then to the electrode surface. Also, by illumination in the Soret-band region, especially in the back-side mode, no change of anodic photocurrents is observed. The quantum yields for anodic photocurrents under the back-side illumination were calculated to be 1.15 and 1.53% at 740 and 400 nm, respectively, which are quite higher as compared to those for the ZnNc electrode.

At the electrode surface the hole carriers transported through ZnTQP oxidize HQ to BQ in the electrolyte. For the carrier transfer from the ZnTQP surface to HQ, the valence band of ZnTQP should be at an appropriate energy level with respect to the redox potential of HQ/BQ. Therefore, the photooxidation reaction should depend on the pH value of the electrolyte solution. Figure 9 shows the pH dependence of the anodic photocurrents at E_{rest} in the dark (0.35 V vs Ag/AgCl) for the ZnTQP electrode under monochromatic illumination from the back side at the Soret-band (400 nm) and the Q-band (680 nm) absorptions. The dashed line in the figure indicates the redox potential ($E_{HQ/BQ}$) of the HQ/BQ solution measured vs Ag/AgCl with a Pt electrode. Maximum photocurrents are obtained at pH 4 for the Soret-band illumination and at pH 8.5 for the Q-band one. It demonstrates that the photooxidation reactions corresponding to the Soret- and Q-band excitations occur separately; i.e. the valence-band edges for the Soret and Q bands are at different potentials, respectively.

Discussion

Detailed consideration of processes such as exciton formation, charge separation to carriers, and carrier transfer to the interface with the electrolyte solution is not the subject of this paper and is only fundamentally mentioned in reference to some relevant literature. In addition, it should be mentioned that the photocurrent efficiency of phthalocyanine-modified electrodes is influenced by morphology and molecular orientation.[25,49] But the positions of energy levels and p- and n-type characters are properties of each material and are therefore not affected by the electrode morphology.[25] Therefore the photoelectrochemical behavior of ZnNc and ZnTQP electrodes prepared by different methods can be discussed here in terms of the energy configuration of dye layers and electrolyte solution, as is depicted in Figure 10. The relative positions of the HOMO and LUMO energies were referred to the UPS and VIS spectroscopic data. When the energy positions determined from UPS are referred to the electrochemical

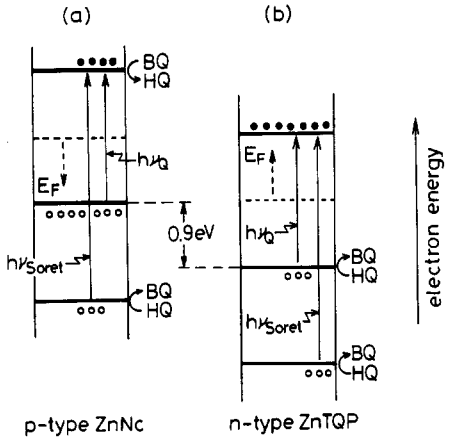

Figure 10. Schematic energy configurations for ZnNc (a) and ZnTQP (b) electrodes.

scale using the usual relation that 0 V vs NHE is equivalent to −4.5 to −4.7 eV vs vacuum,[50,51] an absolute energy mismatch is obvious. This mismatch may arise not only from a surface polarization as a result of a contact with the electrolyte, but also from the fact that the HOMO levels of ZnNc and ZnTQP were referred to the Fermi edge of gold which was independently measured by UPS. However, conclusions drawn from relative trends observed in both electrochemical and UPS scales lead to reasonable results. Further refinement of the absolute energy position is under investigation by UPS measurements using the Fermi edge of gold which was simultaneously deposited on the specimen film without breaking the vacuum.

Photooxidation at the ZnTQP electrode, in contrast to photoreduction at the ZnNc electrode, which is attributed to the p-type semiconductor/electrolyte contact, may simply remind us that the ZnTQP film has n-type semiconducting characteristics. Such n-type molecular semiconductions have also been reported for photoelectrochemical processes of perylene dye thin films.[52] Photovoltaic effects observed for a Schottky cell of Al/tetrapyridylporphyrin/ITO have also been explained in terms of the n-type semiconduction of the tetrapyridylporphyrin film.[26] Our previous photoelectrochemical investigations for Pc derivatives have proposed a similar change of the semiconduction type due to substitution with pyrido and pyrazino groups into the Pc ligand.[17,25] Furthermore, thermoelectric power measurements have recently suggested opposite conduction types for ZnNc and ZnTQP.[53] In the I–V curves of the ZnNc electrode (Figure 5) anodic dark currents are not influenced by illumination, while cathodic currents are increased by illumination. It suggests that the number of holes in the HOMO of ZnNc cannot be significantly changed by illumination (p-type). On the other hand, the I–V curves of ZnTQP (Figure 7) indicate that the number of electrons in the LUMO is not significantly changed by illumination (n-type), but holes are excited in the HOMO under illumination to produce high anodic photocurrents. As is demonstrated by the UPS measurements, the HOMO energy of ZnTQP is lower than that of ZnNc by ca. 0.9 eV. It suggests that in the HOMO–LUMO band gap of ZnTQP, which is estimated to be ca. 1.7 eV from the VIS spectrum (Figure 3c), a larger number of the trap states possibly exist in lower energy as compared to the case for ZnNc. In contact with the ambient, metal, or semiconductor substrates, these lower energy states in ZnTQP could give rise to the donor electrons in the band gap.

In the solid state of molecular semiconductors, the weak intermolecular interaction forms narrow energy bands.[22] Therefore, it can be said that the energetic states in the valence bands, corresponding to the Soret- and Q-band transitions, respectively, are separated in the films, as is seen also in absorption spectra and shown in Figure 10. Both the Soret and Q bands, after excitation, contribute to the photocurrents (Figures 6 and 8). The photocurrent action spectra of the ZnTQP electrode (Figure 8), which show anodic photocurrents well-matched to the VIS spectra for both the Soret- and Q-band absorptions under the back-side illumination, suggest that the valence-band edges of both the Soret and Q bands are in appropriate levels with respect to the energy distribution of HQ in the electrolyte to give rise to the photooxidation in that condition. Therefore, a change in the $E_{HQ/BQ}$ position of the electrolyte relative to the valence-band edges influences their anodic photocurrents. The pH dependence of the anodic photocurrents for ZnTQP (Figure 9) exhibits different $E_{HQ/BQ}$ positions for the optimum energy configurations between the valence-band edges and the HQ distribution, respectively, under the Soret- and Q-band illuminations. However, the potential difference for the optimum photooxidation at the Q and Soret bands, ca. 0.12 V, is much smaller than would be expected from the energy difference of 1.3 eV in their optical absorptions. Only a small part of the initially higher oxidation power of holes in the sub-HOMO orbital can be preserved until charge transfer to the electrolyte occurs. The difference is lost during relaxation of the holes into more stable states, most probably surface states. At Pc electrodes a similar mechanism for excited electron relaxation has been proposed[12,54] and could be confirmed by potential-dependent impedance measurements.[55] It could be attributed to different surface states which are distributed within the band gaps corresponding to the Soret and Q bands, respectively.

As seen in the photocurrent action spectra of the ZnTQP electrode (Figure 8), the back-side illumination produced much higher anodic photocurrents than front-side illumination. Two possible reasons are expected for this behavior: a photoactive contact at the ITO/ZnTQP interface and a morphological effect of the ZnTQP layer. The ITO/ZnTQP contact can give rise to an electron flow from ITO into the ZnTQP layer because the electron trap states in the ZnTQP film possibly lie under the degenerated states of ITO due to its low absolute energy positions. Thus, space-charges diffused at the ITO/ZnTQP interface form a potential gradient to produce anodic photocurrents at the ZnTQP electrode. If this is the case, the front-side illumination should indicate the optical filtering effect. The photocurrent action spectrum under the front-side illumination (Figure 8) really exhibits reduced photocurrents; however, it does not show a clear filtering effect but anodic photocurrents still higher in the Q-band absorption region. This is in contrast with a clear filtering effect, as observed for the ZnNc electrode under the back-side illumination (Figure 6). The morphology of the drop-casted ZnTQP layer is rather rugged and cracked as compared to the homogeneous ZnNc vacuum-deposited film (Figure 2). This discontinuous structure of the ZnTQP layer may cause a penetration of the electrolyte into the layer. Therefore, the back-side illumination can excite the ZnTQP crystallites which are in good contact with the ITO substrate and electrolyte solution. This is the case even if the pigment/electrolyte contact produces the photocurrent and an illumination from the back side yields a higher current because transport of charge carriers to the back electrode is improved. In the present situation it is therefore not possible to exclude one or the other of the two effects.

On the other hand, the electrochemical behavior of the ZnNc electrode was interpreted as follows. The I–V curve in the dark (Figure 5) suggests that the ZnNc film forms nearly ohmic contacts with the ITO substrate and electrolyte solution. In comparison to ZnPc, which showed a typical rectifying I–V curve in the same electrochemical condition due to the blocking contact between the p-type semiconducting ZnPc layer and the electrolyte,[25] the extended π-electron conjugating macrocyclic system in the Nc ligand gives rise to an elevation of both the HOMO and LUMO energy levels as demonstrated by the UPS measurements. These higher energy states are unfavorable for an electron injection from the electrolyte or ITO into the ZnNc layer to form

a blocking space-charge layer at the ZnNc/electrolyte or ITO/ZnNc interface. Under illumination this nearly ohmic contact produces only small cathodic photocurrents (Figure 5). The photocurrent action spectra (Figure 6) indicate that those cathodic currents are only enhanced under the front-side illumination at the Q-band absorption, whereas the illumination at the Soret-band absorption produces oppositely anodic photocurrents. The cathodic photocurrents at the Q-band can be attributed to the HOMO–LUMO excitation and to subsequent electron transfer from the LUMO state of ZnNc into BQ which is likely mediated via surface states existing in the band gap.[6] On the other hand, the anodic photocurrents at the Soret band should be attributed to a hole injection from the underlying sub-HOMO, corresponding to the Soret-band excitation, into HQ in the electrolyte solution. Before illimination, there must be no holes in the sub-HOMO state. Holes in the HOMO only contribute to anodic dark currents. It is expected that under the Soret-band illumination "hot holes" generated in the sub-HOMO state directly oxidize HQ, and that this hole injection obviously occurs fast enough to compete with the excited-state relaxation.

To conclude, the present study has demonstrated that the energetic positions of the HOMO and LUMO levels in the dye molecules are very essential to dominate their semiconducting properties such as p- and n-type behaviors, respectively. For structurally related phthalocyanine and substituted tetraazaporphyrins, it had been shown by photoelectrochemical,[17,25] photovoltaic,[9-11] and thermoelectric power measurements.[53] The lowering of the HOMO and LUMO energy levels in ZnTQP due to substitution with electron-localizing quinoxalino groups tends to prevent acceptor impurities such as oxygen from accepting charges from the dye molecules, and therefore, it probably decreases the p-type semiconducting nature, as compared to ZnNc. On the other hand, some electron-donating impurities in ZnTQP might originate in donor states in the band gap, i.e. result in n-type semiconduction. To study the conduction type in the molecular semiconducting materials, further molecular modifications with electron-withdrawing or electron-donating substituents and with different molecular framework are in progress, and the energy configuration, such as the HOMO and LUMO levels of the dye molecules, the work function of substrate electrodes, and the potential of included redox species, should be considered in detail.

Acknowledgment. The authors would like to thank R. Wahlster, Institute für Organische und Makromolekulare Chemie, Universität Bremen, for her helpful suggestions and discussion on the synthesis of the materials.

References and Notes

(1) Chapin, D. M.; Fuller, C. S.; Pearson, G. L. *J. Appl. Phys.* **1954**, *25*, 676.
(2) Kalvin, M. *Acc. Chem. Res.* **1978**, 11.
(3) Berezin, B. D. *Coordination Compounds of Porphyrins and Phthalocyanines*; J. Wiley & Sons: New York, 1981.
(4) Dorarent, J. R.; Donglor, P.; Harrison, A.; Porter, G.; Rickonf, M.-C. *Coord. Chem. Rev.* **1982**, *44*, 83.
(5) Leznoff, C. C., Lever, A. B. P. *Phthalocyanines; Properties and Applications*; VCH-Publishers: New York, 1989.
(6) Giraudeau, A.; Fan, F.-R.; Bard, A. J. *J. Am. Chem. Soc.* **1980**, *102*, 5137.
(7) Vlachopoulos, N.; Liska, P.; McEvoy, A. J.; Grätzel, M. *Surf. Sci.* **1987**, *189/190*, 823.
(8) Chamberlain, G. A. *Solar Cells* **1983**, *8*, 47.
(9) Tang, C. W. *Appl. Phys. Lett.* **1986**, *48*, 183.
(10) Wöhrle, D.; Meissner, D. *Adv. Mater.* **1991**, *3*, 129.
(11) Kampas, F. J.; Yamashita, K.; Fajer, J. *Nature* **1980**, *284*, 40.
(12) Loutfy, R. O.; McIntyre, L. F. *Can. J. Chem.* **1983**, *61*, 72.
(13) Klofta, T. J.; Rieke, P. C.; Linkous, C. A.; Buttner, W. J.; Nanthakumar, A.; Mewborn, T. D.; Armstrong, N. R. *J. Electrochem. Soc.* **1985**, *132*, 2134.
(14) Klofta, T. J.; Danziger, J.; Lee, P. A.; Pankow, J. W.; Nebesny, K. W.; Armstrong, N. R. *J. Phys. Chem.* **1987**, *91*, 5646.
(15) Schlettwein, D.; Kaneko, M.; Yamada, A.; Wöhrle, D.; Jaeger, N. I. *J. Phys. Chem.* **1991**, *95*, 1748.
(16) Simon, J.; André, J. J. *Molecular Semiconductors*; Springer Verlag: Berlin, 1985.
(17) Schlettwein, D.; Jaeger, N. I.; Wöhrle, D. *Ber. Bunsen-Ges. Phys. Chem.* **1991**, *95*, 1526.
(18) Harrison, S. E.; Ludewig, K. H. *J. Chem. Phys.* **1966**, *45*, 343.
(19) Tachikawa, H.; Faulkner, L. R. *J. Am. Chem. Soc.* **1979**, *100*, 4379.
(20) Harrison, S. E. *J. Chem. Phys.* **1969**, *50*, 4739.
(21) Schlettwein, D.; Armstrong, N. R.; Lee, P. A.; Nebesny, K. W. *Mol. Cryst. Liq. Cryst.*, Submitted for publication.
(22) Orti, E.; Bredas, J. L.; Clarisse, C. *J. Chem. Phys.* **1990**, *93*, 1228.
(23) Fierro, C.; Anderson, A. B.; Scherson, D. A. *J. Phys. Chem.* **1988**, *92*, 6902.
(24) Hale, P. D.; Pietro, W. J.; Ratner, M. A.; Ellis, D. E.; Marks, T. J. *J. Am. Chem. Soc.* **1987**, *109*, 5943.
(25) Yanagi, H.; Tsukatani, K.; Yamaguchi, H.; Ashida, M.; Schlettwein, D.; Wöhrle, D. *J. Electrochem. Soc.* **1993**, *140*, 1942.
(26) Yamashita, K.; Harima, Y.; Matsubayashi, T. *J. Phys. Chem.* **1989**, *93*, 5311.
(27) Mikhalenko, S. A.; Luk'yanets, E. A. *Zh. Obshch. Khim.* **1969**, *39*, 2554.
(28) Wheeler, B. L.; Nagasubramanian, G.; Bard, A. J.; Schechtman, L. A.; Dininny, D. R.; Kenny, M. E. *J. Am. Chem. Soc.* **1984**, *106*, 7404.
(29) Wöhrle, D.; Gitzel, J.; Krawczyk, G.; Tsuchida, E.; Ohno, H.; Okura, I.; Nishisaka, T. *J. Makromol. Sci. Chem.* **1988**, *A25*, 1227.
(30) Kaplan, M. L.; Lovinger, A. J.; Reents, W. D., Jr.; Schmidt, P. H. *Mol. Cryst. Liq. Cryst.* **1984**, *112*, 345.
(31) Bloom, A.; Burke, W. J. *U.S. Patent No. 4* **1980**, *241*, 355.
(32) Van der Veen, J.; Kivits, J.; De Bont, M. R. J. *U.S. Patent No. 4* **1981**, *98*, 975.
(33) Yanagi, H.; Kouzeki, T.; Ashida, M.; Noguchi, T.; Manivannan, A.; Hashimoto, K.; Fujishima, A. *J. Appl. Phys.* **1992**, *71*, 5146.
(34) Rothkopf, H. W.; Wöhrle, D.; Müller, R.; Kossmehl, G. *Chem. Ber.* **1975**, *108*, 875.
(35) Edwards, L.; Goutermana, M. *J. Mol. Spectrosc.* **1970**, *33*, 292.
(36) Lucia, E. A.; Verderame, F. D. *J. Chem. Phys.* **1968**, *48*, 2674.
(37) Schlettwein, D.; Jaeger, N. I.; Wöhrle, D. *Makromol. Chem.* **1992**, *59*, 267.
(38) Manivannan, A.; Nagahara, L. A.; Hashimoto, K.; Fujishima, A.; Yanagi, H.; Kouzeki, T.; Ashida, M. *Langmuir* **1993**, *9*, 771.
(39) Yanagi, H.; Kouzeki, T.; Ashida, M. *J. Appl. Phys.* **1993**, *73*, 3812.
(40) Schaffer, A. M.; Gouterman, G.; Davidson, E. R. *Theor. Chim. Acta* **1973**, *30*, 9.
(41) Nush, N. S.; Cheung, A. S. *Chem. Phys. Lett* **1977**, *47*, 1.
(42) Ciliberto, E.; Doris, K. A.; Pietro, W. J.; Reisner, G. M.; Ellis, D. E.; Fragala, I.; Herbstein, F. H.; Ratner, M. A.; Marks, T. J. *J. Am. Chem. Soc.* **1984**, *106*, 7748.
(43) Klofta, T. J.; Sims, T. D.; Pankow, J. W.; Danziger, J.; Lee, P. A.; Nebesny, K. W.; Armstrong, N. R. *J. Phys. Chem.* **1987**, *91*, 5651.
(44) Berkowitz, J. *J. Chem. Phys.* **1979**, *70*, 2819.
(45) Schlettwein, D.; Wöhrle, D.; Jaeger, N. I. *J. Electrochem. Soc.* **1989**, *136*, 2882.
(46) Höchst, H.; Goldmann, A.; Hüfner, S.; Malter, H. *Phys. Status Solidi b* **1976**, *76*, 559.
(47) Gosh, A. K.; Morel, D. L.; Feng, T.; Shaw, R. F.; Rowe, C. A., Jr. *J. Appl. Phys.* **1974**, *45*, 230.
(48) Fan, F.-R.; Faulkner, L. R. *J. Chem. Phys.* **1978**, *69*, 3341.
(49) Yanagi, H.; Douko, S.; Ueda, Y.; Ashida, M.; Wöhrle, D. *J. Phys. Chem.* **1992**, *96*, 1366.
(50) Royes, R. M. *J. Am. Chem. Soc.* **1962**, *84*, 513.
(51) Gomer, R.; Tryson, G. *J. Chem. Phys.* **1977**, *66*, 4413.
(52) Danziger, J.; Dodelet, J.-P.; Armstrong, N. R. *Chem. Mater.* **1991**, *3*, 812.
(53) Schlettwein, D.; Wöhrle, D.; Karmann, E.; Melville, U. *Chem. Mater.* **1994**, *6*, 3.
(54) Leempoel, P.; Fan, F.-R.; Bard, A. J. *J. Phys. Chem.* **1983**, *87*, 2948.
(55) Fan, F.-R.; Faulkner, L. R. *J. Am. Chem. Soc.* **1979**, *101*, 4779.